Location and Mobility of Ubiquinones of Different Chain Lengths in Artificial Membrane Vesicles†

E. L. Ulrich,‡ M. E. Girvin,§ W. A. Cramer,* and J. L. Markley‡

Departments of Biological Sciences and Chemistry, Purdue University, West Lafayette, Indiana 47907

Received August 15, 1984; Revised Manuscript Received November 28, 1984

ABSTRACT: Ubiquinone (UQ_n with n = 2, 3, or 10 isoprenoid groups) was incorporated into small, sonicated vesicles made of dipalmitoylphosphatidylcholine (DPPC) or dimyristoylphosphatidylcholine (DMPC). (1) The accessibility of oxidized UQ in DPPC or DMPC vesicles to the reductant sodium borohydride ($NaBH_4$), measured by UV spectroscopy, was $UQ_2 > UQ_3 > UQ_{10}$ (DPPC) and $UQ_2 > UQ_3 \sim UQ_{10}$ (DMPC). (2) Catalysis of the reduction of entrapped ferricyanide by exogenous $NaBH_4$ was more effective with UQ_2 than UQ_{10} but was slower with all quinones than reduction by added dithionite. (3) The methoxy protons of UQ_2 and UQ_3 in DPPC and DMPC vesicles exhibited a single NMR resonance centered at ~3.95 ppm, whereas the methoxy groups of UQ_{10} gave rise to two separate proton resonances, at 3.93 ppm and a more narrow resonance at 3.78 ppm. The UQ_{10} population characterized by the 3.78 ppm resonance was present at a higher concentration in DPPC than in DMPC vesicles and was relatively insensitive to reduction by $NaBH_4$. (4) UQ_{10} perturbed the melting temperature (T_m) of DPPC vesicles to a smaller extent (ΔT_m = −1 °C) than did UQ_2 and UQ_3 (ΔT_m = −3 to −4 °C). The combined UV and NMR data imply the following: The UQ_{10} pool characterized by the 3.78 ppm peak corresponds to a more mobile UQ_{10} fraction that is not reduced by $NaBH_4$ in 2–3 min and is thought to be localized close to the center of the DPPC bilayer since it has little effect on the DPPC T_m. The population of UQ_{10} in DPPC vesicles corresponding to the 3.93 ppm peak would then correspond to the UQ_{10} pool that is reduced slowly by $NaBH_4$ and is located in a bilayer environment magnetically similar to that of UQ_2 and UQ_3. UQ_2 appears to be positioned near the bilayer surface because of its accessibility to $NaBH_4$ and relatively large effect on the lipid T_m. The distribution of UQ_3 according to the kinetic data is intermediate between that of UQ_2 and the UQ_{10} pool near the bilayer center, although the magnetic environment of UQ_3 appears the same as that of UQ_2. Physiological activities often require quinones with long isoprenoid chains. The present data argue against transmembrane "flip-flop" of long-chain quinones. It is proposed that one essential property of the long-chain quinones for transfer of electrons and protons across the bilayer is their residence in the hydrophobic core.

Mechanisms by which physiological quinones carry protons through respiratory and photosynthetic electron-transport chains and across membranes, as postulated in the chemiosmotic models of the respiratory and photosynthetic electron-transport chain (Mitchell, 1966, 1976), have been discussed extensively [e.g., see Crane (1977), DePierre & Ernster (1977), Trumpower (1981), and Hauska & Hurt (1982)]. Ubiquinone 10 (UQ_{10})[1] in the straight-chain trans configuration has a length of 56 Å, greater than the thickness of a phospholipid bilayer (Trumpower, 1981). The arrangement of the long prenyl chains in the membrane poses an obvious structural problem for the proposed transmembrane motion of UQ_{10} and PQ_9 in respiratory and photosynthetic membranes. The position of PQ_9 in the membrane has also become important in understanding the mechanism of long-range electron transfer from photosystem II to photosystem I in chloroplasts (Anderson, 1981).

A primary approach to studies of quinone function has been the comparison of functional and structural properties of quinones having different prenyl chain lengths. Reconstitution studies of electron-transport activity in mitochondria, chromatophores, and *Escherichia coli* have shown a requirement for ubiquinone with at least three isoprenoid units: (i) UQ_8–UQ_{10} was much more efficient than UQ_0–UQ_2 in restoring NADH oxidase activity in reconstituted solvent-extracted heart mitochondria, whereas UQ_3–UQ_7 exhibited intermediate activity (Crane, 1977; Lenaz et al., 1981). However, all UQ_n compounds except UQ_0 and UQ_1 were active in restoring succinate oxidase activity in the presence of an added lipid fraction (Crane, 1977; Crane & Ehrlich, 1960). (ii) Phosphorylation as well as electron-transport activity in UQ_{10}-depleted chromatophores was restored to the same extent [~180 μmol of ATP (mg of BChl)$^{-1}$ h^{-1}] with UQ_3 as with UQ_{10}, but UQ_1 and UQ_2 were much less active (Baccarini-

†This work was supported by Grants PCM-8022807 and PCM-8403308 from the National Science Foundation (to W.A.C.), Grant 9-8482-CRCR-1-1045 from the U.S. Department of Agriculture, Cooperative State Research Service, Science and Education (to J.L.M. and E.L.U.), and Grant RR01077 from the Biotechnology Resources Program of the Division of Research Resources, National Institutes of Health, for the Purdue University Magnetic Resonance Laboratory (to J.L.M.). M.E.G. was the recipient of National Institutes of Health Predoctoral Traineeship GM-07211. Preliminary accounts of this research have been presented (Ulrich et al., 1982, 1983).

*Address correspondence to this author at the Department of Biological Sciences, Purdue University.

‡Present address: Department of Biochemistry, University of Wisconsin—Madison, Madison, WI 53706.

§Present address: Department of Physiological Chemistry, University of Wisconsin—Madison, Madison, WI 53706.

[1] Abbreviations: DPPC, dipalmitoylphosphatidylcholine; DMPC, dimyristoylphosphatidylcholine; UV, ultraviolet; T_m, midpoint temperature of the gel → liquid-crystalline lipid phase transition; BChl, bacteriochlorophyll; UQ_n and PQ_n, ubiquinone and plastoquinone with n isoprenoid groups; MOPS, 3-(*N*-morpholino)propanesulfonic acid; DSS, 4,4-dimethyl-4-silapentanesulfonic acid; Me_4Si, tetramethylsilane; Tricine, *N*-[tris(hydroxymethyl)methyl]glycine.

0006-2960/85/0424-2501$01.50/0

Melandri et al., 1980). (iii) UQ_3–UQ_8 were also more efficient than UQ_1 and UQ_2 at reconstituting NADH oxidase activity in vesicles prepared from an *E. coli* double quinone mutant, although D-lactate-driven proline transport was restored by lower concentrations of UQ_1 than UQ_8 (Stroobant & Kaback, 1979). (iv) Efficient electron transport across artificial asolectin membranes catalyzed by incorporated UQ_n showed a chain length requirement of at least three isoprenoid units (Futami et al., 1979).

The ring of UQ_{10} in mitochondrial membranes is known to be inaccessible to hydrophilic donors and acceptors (Crane, 1977). These data and those on reconstitution of mitochondrial membrane function led Crane (1977) to suggest a possible model for the orientation of UQ_{10} in lipid bilayers in which the quinone ring and the prenyl chains are in the center of the lipid bilayer with the ring in the plane of the membrane and perpendicular to the lipid fatty acid chains. A similar model was recently proposed again, mainly as a result of studies of the surface activity of quinone and lipid monolayers (Quinn & Esfahani, 1980) and calorimetry and fluorescence probe measurements of quinones in DPPC vesicles (Alonso et al., 1981; Katsikas & Quinn, 1981, 1982). It was also inferred that the long-chain quinones reside in the center of the lipid bilayer in concentrated domains in which the lifetime of the semiquinone would be small, since UQ_1 incorporated into asolectin vesicles could be reduced to the semiquinone state by externally added dithionite, whereas the semiquinone was not formed by dithionite addition to incorporated long-chain quinone (Futami & Hauska, 1979). This view of preferential location of long-chain quinones in the bilayer center differs from or modifies the more traditional view that transmembrane "flip-flop" of long-chain quinones across membranes provides the mechanism for quinone-catalyzed electron and proton transport [e.g., see Mitchell (1966, 1976), Hauska & Hurt (1982), and Kingsley & Feigenson (1981)].

The purpose of the present study was to determine the relative position of long- and short-chain quinones in chemically defined liposomal membranes and their role in catalyzing transmembrane electron transport.

Experimental Procedures

Materials. DMPC and DPPC were obtained from Sigma. Ubiquinones were gifts from Professor F. L. Crane and the Eisai Co., Tokyo, Japan.

Vesicle Preparation. Lipids and quinones were dissolved in $CHCl_3$ and stored at −20 °C. Quinone concentrations were determined from absorption spectra at 275 nm minus 300 nm by using the extinction coefficient of UQ_{10}, 14.3 mM^{-1} (Barr & Crane, 1971). A mixture of the quinone and 5–10 mg of lipid was dried to a thin film in a small test tube by rotating the tube under a stream of nitrogen. When the film was completely dried, 0.4 mL of 0.1 M KCl and 10 mM buffer, either phosphate (pH 7) for NMR or Tricine (pH 8.0 or 8.8) for optical spectroscopy, was added. The resulting suspension was sonicated to clarity in a Branson bath sonicator for 15–30 min at a temperature 10–15 °C above the melting temperature of the lipid. The buffer solvent was ^2H_2O (99.75 mol %, Bio-Rad) for the NMR measurements.

Vesicles containing trapped ferricyanide were prepared by using the procedure of Futami et al. (1979). Vesicles were prepared as described above, but the buffer contained 50 mM Tricine, pH 8.0 or 8.8, and 0.2 M ferricyanide. After sonication, the vesicles were passed through a 1.5 × 20 cm Sephadex G-50 column at 52 °C to remove external ferricyanide.

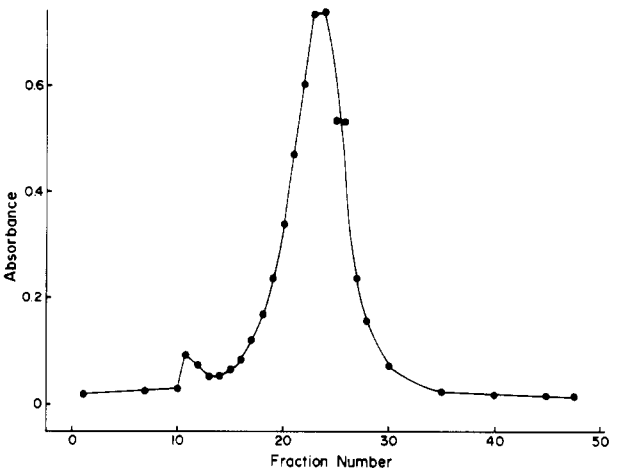

FIGURE 1: Elution profile for DPPC vesicles containing 2 mol % UQ_{10}. 20 mg of DPPC and 0.5 mg of UQ_{10} were cosonicated in 0.8 mL of 0.1 M KCl and 10 mM Tricine, pH 8.8. The vesicles were loaded onto a 1.5 × 26 cm Sepharose 2B column at 52 °C, and fractions of 1 mL were collected.

Vesicle Homogeneity. The homogeneity of the vesicles used in the spectroscopic studies was determined by eluting DPPC vesicles containing 1–5 mol % UQ_{10} through a 1.5 × 26 cm Sepharose 2B column equilibrated at 52 °C, with the absorbance of 1-mL fractions monitored at 275 nm. The phospholipid concentration was determined according to Rouser et al. (1966). The quinone was seen to elute in one major band with a small shoulder that contained <10% of the total quinone (Figure 1); the homogeneity of the vesicles was substantially greater than that reported in previous NMR experiments on this subject (Kingsley & Feigenson, 1981). Vesicles used for all UV or visible spectroscopic measurements contained 1 mol % UQ_n, and those used for NMR studies contained 5 mol % unless otherwise noted. Typical values in energy-transducing membranes are approximately 1–3 mol % relative to the lipid (Hauska & Hurt, 1982).

Measurement of Quinone and Ferricyanide Reduction. Reduction of the quinones incorporated into bilayer vesicles was followed in an Aminco-Chance dual-wavelength spectrophotometer using 275 nm as the sample wavelength and 300 nm as the reference with $NaBH_4$ as a UV-transparent reductant. The cuvette was stirred and thermostated at 32 and 52 °C, respectively, for DMPC and DPPC lipid vesicles. Twenty microliters of the vesicle suspension was added to 2.5 mL, with a final concentration of 270 μM DPPC and 2.7 μM (1 mol %) or 14 μM (5 mol %) quinone. A relatively dilute final concentration of $NaBH_4$, usually 0.4 mM, was used so as to minimize the formation of bubbles in the cuvette, especially at higher temperatures. Since $NaBH_4$ is known to be more stable to hydrolysis when in alkaline solution (Brown & Swensson, 1957), it was used at the highest possible pH at which the quinones were stable to autoxidation. The reducing ability of borohydride was approximately constant for at least 3 min as measured in the presence of redox buffers with a redox electrode. The total amount of quinone present in the vesicles was measured by the difference in absorbance at 275 vs. 300 nm in a complete spectrum of the original vesicles before addition of $NaBH_4$. For ferricyanide reduction, 0.2 mL of the vesicle eluant from the G-50 column was added to 2.5 mL in the cuvette, and the wavelength pair, 420–480 nm, was used to assay reduction.

NMR Spectroscopy. ^1H NMR spectra were obtained with a Nicolet Magnetics 10.7 T NT-470 spectrometer operating in the pulse Fourier transform mode. The temperature of the

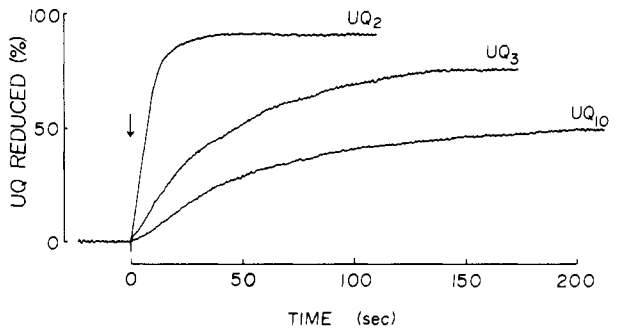

FIGURE 2: Time course of reduction of UQ_n in DPPC vesicles by $NaBH_4$ (0.4 mM) at 52 °C. Quinone concentrations were 2.7 μM or 1 mol % relative to DPPC. Solutions contained 0.1 M KCl and 10 mM Tricine buffer at pH 8.8.

Table I: Reduction by Borohydride of UQ_n in DPPC and DMPC Vesicles[a]

	(A) DPPC		(B) DMPC	
	UQ reduced (%)	initial rate (nM UQ/s)	UQ reduced (%)	initial rate (nM UQ/s)
UQ_2	94 ± 5	260 ± 3	82 ± 3	166 ± 8
UQ_3	76 ± 5	55 ± 0	77 ± 2	21 ± 1
UQ_{10}	44 ± 3	22 ± 0.2	67 ± 0	17 ± 1

[a] Reduction by 0.4 mM BH_4^- at pH 8.8 at 52 and 32 °C, respectively, of UQ_n (1 mol %) in DPPC and DMPC vesicles. Errors are the range of values from three to four experiments.

probe was calibrated with a methanol thermometer (Van Geet, 1968). Chemical shifts are reported in parts per million (ppm) from an internal reference standard, either tetramethylsilane (Me_4Si) for nonaqueous solvents or 4,4-dimethyl-4-silapentanesulfonic acid sodium salt (DSS), used in aqueous solvents at a concentration of 0.4 mM in all samples to minimize possible errors due to partitioning of the reference compound in the lipid phase.

RESULTS

Differential Accessibility of Ubiquinone in Liposomes to Reductant. Measurement of the rate of reduction of oxidized UQ_n incorporated into bilayer vesicles by an added charged reductant provides a simple probe of its relative average accessibility to the aqueous interface. The time course of the aerobic reduction by $NaBH_4$ or UQ_2, UQ_3, or UQ_{10} in DPPC vesicles is shown in Figure 2. Differential reductive effects can be ascribed to accessibility, since the redox potentials of the UQ_n are known to be independent of isoprenoid chain length (Moret et al., 1961), and all of the UQ_n used here are completely reduced in ethanol by the same concentration (0.4 mM) of $NaBH_4$ (data not shown). UQ_2 was relatively accessible to the reductant in terms of both the initial rate (260 nM quinone/s) and extent (94%) of its reduction (Table IA). UQ_3 shows an intermediate situation, while a lower accessibility of UQ_{10} is shown by its reduction to a smaller level (~45%) and by its slower rate (22 nM quinone/s). For UQ_{10}, the rate and extent (44%) of reduction were unchanged (data not shown) when the major liposome band isolated by Sepharose chromatography (Figure 1) was used. Performing the experiments anaerobically, or increasing the quinone concentration to 5 mol %, had no effect on the rate or extent of quinone reduction. A similar pattern of slower reduction by borohydride of UQ_{10} relative to shorter chain quinones was observed in DMPC vesicles (Table IB).

The dependence of the reduction of the different quinones in DPPC vesicles on the concentration of added BH_4^- also showed UQ_2 to be more accessible than UQ_{10} (Figure 3). The

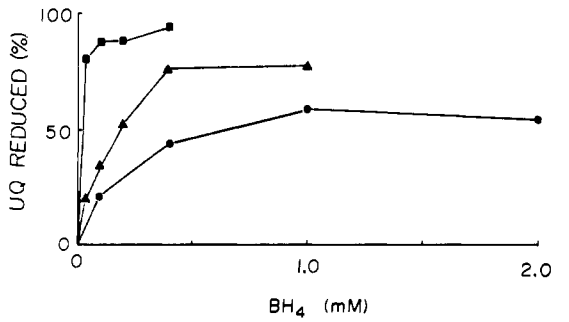

FIGURE 3: Quinone reduction as a function of sodium borohydride concentration. Conditions as in Figure 2. (■) UQ_2; (▲) UQ_3; (●) UQ_{10}. Samples were incubated for 3 min in $NaBH_4$.

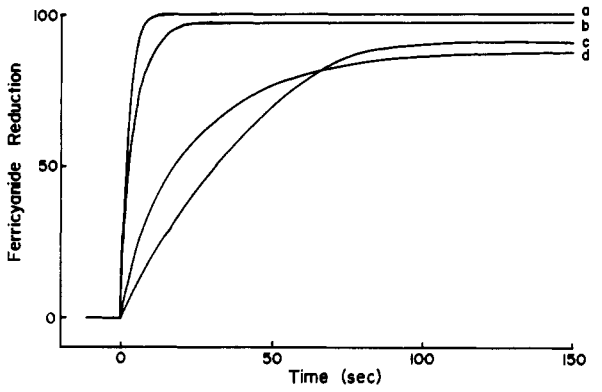

FIGURE 4: Time course for reduction of entrapped ferricyanide by dithionite (0.4 mM) added to DPPC liposomes containing 1 mol % UQ_n: UQ_{10} (a); UQ_3 (b); control (c); UQ_2 (d); pH 8.0. Conditions otherwise as under Experimental Procedures.

reduction was measured after a 3-min incubation with the indicated BH_4^- concentration. Reduction of UQ_2 and UQ_{10} attained a maximum value at 0.1 mM and 1.0 mM $NaBH_4$, respectively, while UQ_3 showed intermediate accessibility, reaching a plateau at 0.4 mM $NaBH_4$. At a concentration of 40 μM $NaBH_4$, 80% of the UQ_2 was reduced, compared to only 20% reduction of UQ_3 and ~5–10% reduction of UQ_{10}. It was not possible to use $NaBH_4$ at concentrations >1–2 mM with DPPC vesicles, or to extend the measurement beyond 3 min, because of spectrophotometric noise arising from bubbles formed at the higher temperature (52 °C).

Reduction of Entrapped Ferricyanide. The ability of added borohydride to reduce ferricyanide entrapped in DPPC vesicles was compared to that of dithionite. The pattern of reduction by dithionite [active reducing species, SO_2^-, at pH 8.0 (Lambeth & Palmer, 1973)] of ferricyanide trapped inside DPPC vesicles containing the different UQ_n compounds was similar (Figure 4) to that measured by Futami et al. (1979) with asolectin vesicles. The rate of ferricyanide reduction in vesicles containing UQ_2 was only slightly faster than the rate in control vesicles. As previously observed by Futami et al. (1979), although UQ_2 appeared to be more accessible than longer chain UQ_n to dithionite, UQ_3 and UQ_{10} were both much more efficient than UQ_2 in catalyzing ferricyanide reduction in the asolectin vesicles. When $NaBH_4$ was used as the reductant, however, ferricyanide reduction was slower with all quinones (Figure 5). In this case, UQ_2 catalyzed the most complete reduction of internal ferricyanide (70%), UQ_3 again showed an intermediate response, and UQ_{10} gave the smallest effect. Our interpretation of these data (see Discussion) relies on the observation that the amount of ferricyanide reduced by $NaBH_4$ (12%, Figure 5) is much smaller than that reduced by dithionite (91%, Figure 4) in control vesicles without a quinone

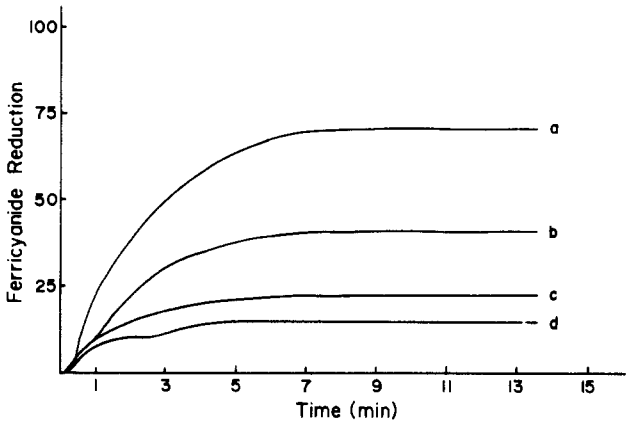

FIGURE 5: Time course for reduction of entrapped ferricyanide by borohydride (0.4 mM, pH 8.8) added to DPPC liposomes containing 1 mol % UQ_n: UQ_2 (a); UQ_3 (b); UQ_{10} (c); control (d). Conditions otherwise as under Experimental Procedures.

catalyst. Dithionite must then be able to penetrate further into the membrane than borohydride or to transfer electrons over a longer distance.

NMR Studies. (A) Existence of Two Environments for UQ_{10} in Lipid Vesicles. Figure 6 shows spectra of UQ_{10} in C^2HCl_3 (Figure 6A), of DPPC vesicles without any incorporated quinone (Figure 6B), and of DPPC vesicles containing UQ_2 (Figure 6C) or UQ_{10} (Figure 6D). Peak assignments are given in the caption to Figure 6. The chemical shift of resonances from UQ_2 or UQ_3 incorporated into DPPC (Figure 6C) or DMPC vesicles (data not shown) is very similar to those of UQ_{10} in C^2HCl_3 (Figure 6A). A comparable spectrum of DPPC or DMPC vesicles containing 5 mol % UQ_{10} (Figures 6D and 7) had resonances at 3.78 and 3.93 ppm, both of which were assigned to the quinone methoxy protons of two different quinone populations (Kingsley & Feigenson, 1981). The methoxy peak at 3.78 ppm, which was not observed until the UQ_{10} concentration reached 2 mol %, comprised about 50% of the total methoxy proton signal at higher UQ_{10} concentrations (Figure 8). Line widths of the two methoxy resonances are 6.4 Hz for the 3.78 ppm peak and about 15 Hz for the 3.93 ppm peak. The chemical shift of the broader peak (3.93 ppm) is similar to that of the single methoxy resonance of UQ_2 (3.96 ppm, Figure 6C) and UQ_3 (3.94 ppm, data not shown) in vesicles. The chemical shift and line width data indicate that UQ_{10} in lipid vesicles exists in two environments, one similar to that occupied by UQ_2 and UQ_3 and the other characterized by a resonance at higher field whose narrower line width is indicative of a higher mobility. Physical exchange of UQ_{10} between these two environments is slow on the NMR time scale ($t_{1/2}$ at least 10 times greater than 14 ms). The amount of UQ_{10} in the mobile state (3.78 ppm peak) can be measured readily and compared for DPPC and DMPC vesicles from spectra recorded at temperatures below the T_m of these vesicles, where the UQ_{10} methoxy resonances are clearly separated (Figure 8). In DPPC vesicles, 80% of the UQ_{10} is in the more mobile state, but in DMPC vesicles, only 30% of the UQ_{10} is found in this environment.

The methoxy resonances of reduced UQ_{10} are known to have chemical shifts upfield (3.82 and 3.65 ppm, respectively, for the two UQ_{10} populations) from the oxidized quinone methoxy peaks at ~3.93 and 3.78 ppm (Kingsley & Feigenson, 1981). The upfield chemical shift of the two peaks was affected differentially by $NaBH_4$ reduction. Upon addition of $NaBH_4$ (1–10 mM) to DPPC vesicles, the broad 3.93 ppm peak, B, was first seen to decrease in intensity, and concomitantly a new peak, B′, appeared at 3.82 ppm (Figure 9). The intensity

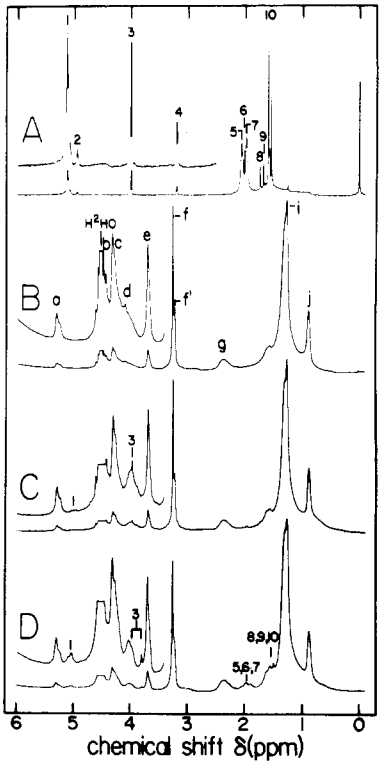

FIGURE 6: ^1H NMR spectra at 470 MHz of (A) UQ_{10} in C^2HCl_3; (B) sonicated DPPC vesicles, and (C and D) sonicated DPPC vesicles with 5 mol % UQ_2 and UQ_{10}, respectively. Spectrum A is the sum of 64 accumulations using 8192 time domain data registers and a recycle time of 4 s at 25 °C. The chemical shifts are referenced to Me_4Si. Sample B was 25 mM in DPPC and 7 mM in phosphate buffer, pH 7.0, and the spectrum sums 16 accumulations using 8192 time domain data registers with a recycle time of 3.8 s at 35 °C. Peak assignments for UQ_{10}, except for the C2′ proton, are from Tsukida (1972): (1) 5.12 ppm, vinyl CH; (2) 4.94 ppm, 2′-vinyl CH, since double resonance experiments (not shown) indicate a coupling to the C1′ proton at 3.19 ppm [this peak had previously been assigned to an impurity (Kingsley & Feigenson, 1979)]; (3) 3.99 and 3.98 ppm, $-OCH_3$; (4) 3.19 ppm, 1′-CH_2; (5) 2.06 ppm, $CH_2CH{=}C$; (6) 2.01 ppm, methyl at C2; (7) 1.97 ppm, $CH_2C(CH_3){=}CH$; (8) 1.74 ppm, methyl at C3′; (9) 1.68 ppm, terminal *trans*-CH_3; (10) 1.60 ppm, isoprenoid CH_3. The chemical shifts for spectra B and C are referenced to DSS. Peak assignments for DPPC are from Birdsall et al. (1972): (a) glycerol HCOCO; (b) glycerol CH_2OCO (a portion of this resonance is also located near peak c); (c) choline $POCH_2$; (d) glycerol CH_2OP; (e) choline CH_2N; (f and f′) choline $N(CH_3)_3$ resonances from the outer and inner surfaces of the vesicle membrane, respectively; (g) α-CH_2; (h) β-CH_2; (i) acyl CH_2; (j) acyl CH_3. The peak at 4.75 ppm in the DPPC spectrum is assigned to HO^2H, and the peak at 3.3 ppm is due to residual CH_3OH in the sample. Sample C, UQ_2 in DPPC, shows a single methoxy proton resonance (3) at 3.96 ppm, and sample D, UQ_{10} in DPPC, shows two methoxy proton resonances at 3.93 and 3.78 ppm. Samples C and D were run under the same conditions as B except for the added UQ_2 or UQ_{10}.

of the sharper peak, S, at 3.78 ppm decreased more slowly as a function of added $NaBH_4$. An overlapping resonance from the choline ($-CH_2N$) protons obscured the high-field methoxy peak of reduced UQ_{10} in the more mobile environment. The reduced quinone peak (3.82 ppm) does not exchange electrons rapidly ($t_{1/2}$ at least 10 times greater than 15 or 53 ms, respectively) with oxidized quinone in either of the pools (3.93 and 3.78 ppm peaks). From the differential reduction of UQ_{10} by $NaBH_4$ in Figures 2 and 3, it is concluded that the 3.93 ppm peak is associated with the UQ_{10} pool that is slowly reduced by $NaBH_4$ (Figures 2 and 3), while the 3.78 ppm resonance is a signature of the inaccessible UQ_{10} fraction that is not seen to be reduced by 2 mM $NaBH_4$ in Figure 3.

(B) Effect of UQ_n on the T_m of the Phase Transition of DPPC Vesicles. Eigenberg & Chan (1980) have shown that

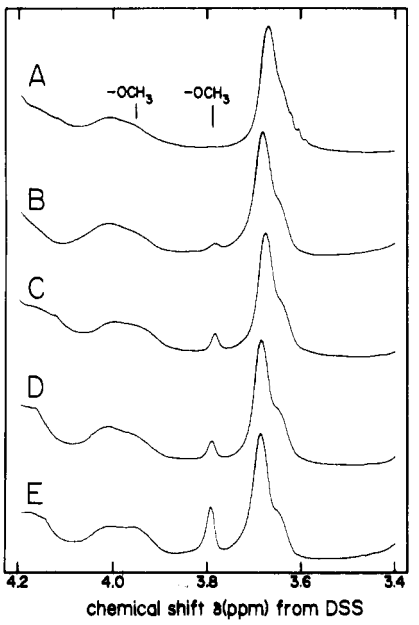

FIGURE 7: ^{1}H NMR spectra of the UQ_{10} methoxy proton resonances as a function of the UQ_{10} concentration in DPPC vesicles. UQ_{10} concentrations were (A) 1%, (B) 2%, (C) 4%, (D) 5%, and (E) 10%. Spectra were collected at 55 °C.

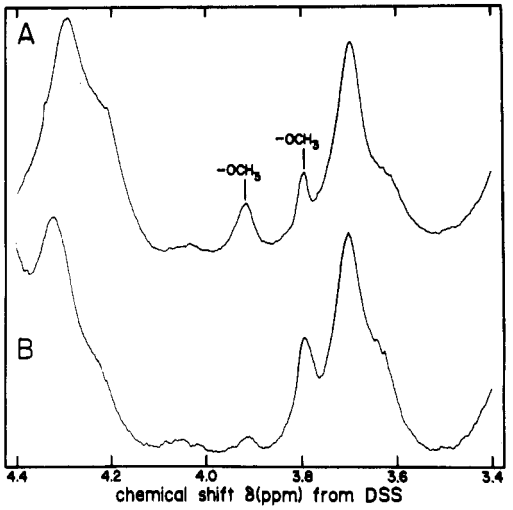

FIGURE 8: Spectra of the UQ_{10} methoxy protons in DMPC (A) and DPPC (B) vesicles. The samples contained 5 mol % UQ_{10}; the spectra were recorded at 10 (A) and 28 °C (B), temperatures below the phase transition of the respective lipid.

the temperature dependence of the chemical shift of the inner choline methyl head group resonance from distearoylphosphatidylcholine vesicles can be used to determine the phase transition temperature of the vesicles. We have found this also to be true for DPPC (Figures 10 and 11) and DMPC (data not shown) vesicles. A third choline methyl resonance appeared in the DPPC vesicle spectrum during the 4–6 h required to obtain a temperature profile (data not shown) and was assigned to lipid in large vesicles formed by fusion of the original smaller vesicles. DPPC vesicles exhibited a T_m of 40 ± 1 °C. The presence of 5 mol % UQ_2 (Figure 11) or UQ_3 (data not shown) lowered the T_m to 36 and 37 °C, respectively. UQ_{10} had a smaller effect on the lipid T_m, shifting it by only about 1 °C to 39 °C (Figure 11). The smaller influence of UQ_{10} on the T_m of DPPC vesicles, relative to that of UQ_2 and UQ_3, is similar to the results obtained by other methods (Alonso et al., 1981; Katsikas & Quinn, 1981, 1982). In contrast, all three quinones had the same effect on the T_m of

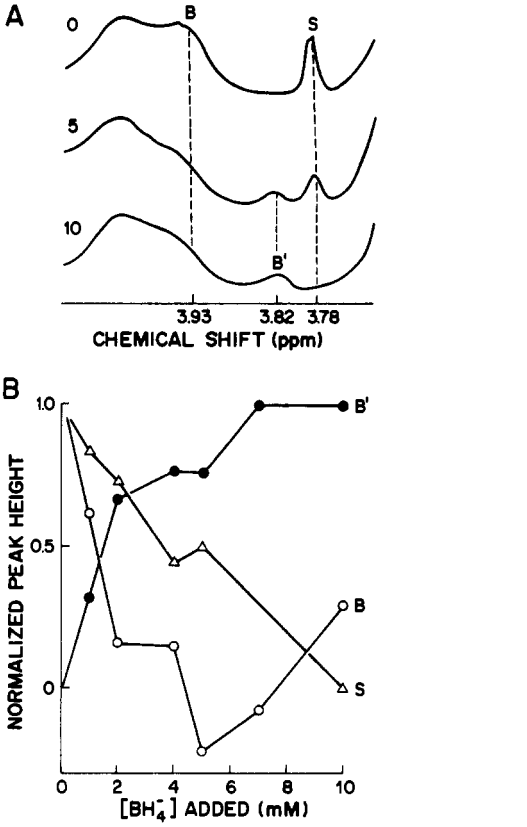

FIGURE 9: Differential reduction by sodium borohydride of the two pools of UQ_{10} in DPPC vesicles. Sodium borohydride was added to each sample to give the initial $NaBH_4$ concentration shown. Spectra were recorded between 15 and 30 min after addition of the reductant according to the spectrometer conditions described for Figure 6D. (A) Representative spectra of the ubiquinone methoxy region. Peak B (broad) is the methoxy signal from oxidized UQ_{10} in the less mobile environment, and peak B' is the methoxy signal from reduced UQ_{10} in this pool. Peak S (sharp) is from oxidized UQ_{10} in the more mobile environment. The signal from reduced UQ_{10} in this pool falls in a crowded spectral region (not shown) and is not resolved clearly. (B) Normalized peak heights of these signals plotted as a function of the initial concentration of added $NaBH_4$. The measured intensity of peak B is subject to some error because the resonance appears as a broad shoulder on a larger peak.

DMPC vesicles, decreasing the T_m by 4–6 °C (data not shown).

The temperature dependence of the spectrum of DPPC vesicles containing 5 mol % UQ_{10} is shown in Figure 10. At 26 °C, well below the lipid phase transition (~40 °C), the DPPC peaks a, b, d, and g of Figure 6B broadened beyond detection. Very broad lipid tail methyl and chain methylene resonances were still observed, as were resonances for the inner and outer choline methyls and outer glycerol ($-CH_2$) protons. Yet, relatively sharp peaks can still be seen at these temperatures for the UQ_{10} chain methyls, methylenes, methine protons, and the high-field methoxy protons. Thus, a significant fraction of the UQ_{10} remains in a pool having a mobile environment below the lipid phase transition.

Discussion

A set of conclusions can be derived from the above UV and ^{1}H NMR spectroscopic data regarding differences in the distributions and mobility of UQ_2 and UQ_{10} at approximately physiological concentrations in the bilayer of DPPC membrane vesicles. Conditions for quinone reduction by sodium borohydride (e.g., 40 μM, 3-min incubation, Figure 3) can be found such that UQ_2 is completely reduced and UQ_{10} is hardly reduced at all. The differential accessibility of UQ_2 and UQ_{10}

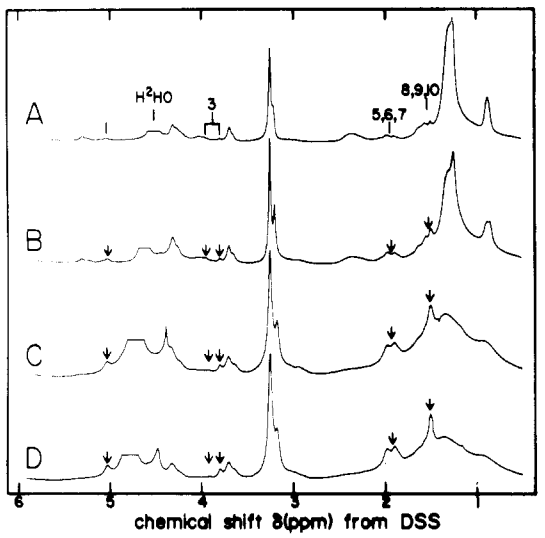

FIGURE 10: ^{1}H NMR spectra of DPPC vesicles containing 5 mol % UQ_{10} as a function of temperature: (A) 52 °C; (B) 40 °C; (C) 32 °C; (D) 26 °C. The spectral parameters were the same as those used for Figure 6D. The errors in (B–D) denote quinone resonances that remain sharp at $T < T_m$.

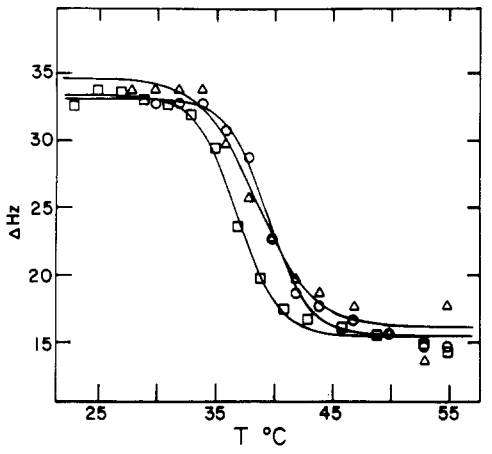

FIGURE 11: Measurement of the lipid phase transition of DPPC vesicles containing 5 mol % UQ: (○) DPPC vesicles; (△) vesicles plus UQ_{10}; (□) vesicles plus UQ_2. The midpoint (T_m) of the transition determined by nonlinear least-squares analysis was 40 °C (vesicles alone), 39 °C (vesicles with UQ_{10}), and 36 °C (vesicles with UQ_2).

to borohydride demonstrates in a simple way the different structural arrangement of the two quinones in DPPC vesicles: Approximately half of the UQ_{10} is positioned deeply enough in the membrane so that it cannot be reached by borohydride within a few minutes, and the other 50% is reduced slowly compared to UQ_2. A position for UQ_{10} in or near the center of the bilayer is also implied by its minimal perturbation of the T_m of DPPC vesicles (Figure 11). Since the location of greatest motion is at the ends of the acyl chains (Stockton et al., 1976), this is the lipid region in which insertion of a hydrophobic compound would least disturb the packing of the lipid molecules and so least affect the T_m of the membrane. A similar model was put forward by Jain & Wu (1977) to explain the lack of any effect on the lipid phase transition profile by many different aromatic hydrocarbon molecules, including the fluorescence probes perylene and diphenylhexatriene, incorporated at high concentration into DPPC vesicles. The existence of the slowly reduced and relatively inaccessible UQ_{10} components, as well as the small extent of UQ_{10}-catalyzed ferricyanide reduction by $NaBH_4$, also implies a slow rate of transmembrane flip-flop motion by UQ_{10}.

Several observations argue against an alternative explanation (Kingsley & Feigenson, 1981) that UQ_{10} forms a separate membrane domain that does not interact with the lipid and may not be located near the center of the bilayer: (1) Interaction of UQ_{10} with the lipid can be inferred from the decrease in the pretransition temperature of the lipid caused by UQ_{10} and, at higher concentrations, of the temperature of the main lipid transition (Katsikas & Quinn, 1981). (2) This point is further substantiated by the observation that the ^{1}H NMR spectrum of the lipid acyl chain terminal methyls is affected by incorporation of UQ_{10} into the bilayer (data not shown). (3) Neither component of the UQ_{10} is reduced readily by BH_4^- (Figures 2 and 3 and Table I), as would be expected if the pool were located at the membrane surface.

In a vesicle system similar to the one used here, except for the use of asolectin instead of DPPC lipid, Futami et al. (1979) measured rates of transmembrane electron transfer from externally added dithionite to internally trapped ferricyanide with different UQ_n species incorporated into the vesicle membrane. With long-chain ubiquinones (UQ_n, $n \geq 3$), the rates were on the order of the rate-limiting step of electron transfer in mitochondria and chloroplasts, while UQ_1 or UQ_2 was not much more efficient than the control without quinone. Similar results were obtained in the present work using dithionite as the external reductant (Figure 4). When BH_4^- was the reductant, however, all the rates were much slower, and only with incorporated UQ_2 was any appreciable amount of ferricyanide reduced (Figure 5). The opposite dependence of reduction efficiency on quinone side chain length for borohydride, as compared to dithionite, is not surprising since only the short-chain quinones are efficiently reduced by BH_4^- (Figures 2 and 3, Table I); if a quinone is not reduced, it cannot reduce any ferricyanide. The much greater rate and extent of ferricyanide (and presumably quinone) reduction by dithionite appear to be a consequence of greater penetration into the liposome membrane or a longer range mechanism of electron transfer (control traces of Figures 4 and 5). Because the net charge on the active reducing species of dithionite, SO_2^- (Lambeth & Palmer, 1973), is the same as that on BH_4^-, the ability of the two reductants to penetrate the membrane should be similar. However, the reduction mechanisms of the two reductants are different. Dithionite as an electron-transfer agent may transfer charge over distances on the order of 10–20 Å (Chance et al., 1979; Poulos & Kraut, 1980). Reduction by BH_4^- involves hydride transfer over a short range after complex formation (House, 1972). Ferricyanide at the high concentration of 0.2 M may penetrate from the inside of the vesicle through the inner half of the bilayer and approach the bilayer center. The limiting step in quinone-mediated reduction of ferricyanide by exogenous reductant would then be transfer of electrons to the bilayer center which dithionite, but not borohydride, could accomplish by long-range electron transfer.

The relatively fast reduction of UQ_2 by $NaBH_4$ (Figure 2) does not distinguish between a static average position of UQ_2 close to the aqueous interface or transmembrane motion of this quinone sufficiently fast to allow it to sample the environment near the membrane surface. However, the data on ferricyanide reduction indicate that UQ_2 crosses the bilayer at a slow rate (Figure 5). The alternative, that UQ_2 causes the vesicles to become slightly leaky toward dithionite and borohydride, is unlikely since Futami & Hauska (1979) have shown that the quinone side chain itself does not increase the vesicle permeability to dithionite. The effect of UQ_2 in decreasing the T_m of DPPC lipid vesicles argues for interaction

of UQ_2 with the lipid close to the membrane surface where the lipid chain motion is smaller (Stockton et al., 1976) and the order parameter greater (Seelig, 1977). Inferences about a surface position of UQ_2 and UQ_3 have been obtained through surface tension, calorimetry, and fluorescence probe measurements (Alonso et al., 1981; Katsikas & Quinn, 1981, 1982) that are in good agreement with the T_m measurements made by the shift of the inside choline methyl head group protons reported here (Figure 11). The distribution of UQ_{10} reported here is more complex than inferred previously but in agreement with the existence of a major centrally located pool. In its accessibility to $NaBH_4$, UQ_3 is intermediate between UQ_{10} and UQ_2. UQ_3 has often been found to be at the transition between the short- and long-chain quinones in its ability to reconstitute physiological electron transport (Baccarini-Melandri et al., 1980; Futami et al., 1979).

The differential effect of UQ_2 and UQ_{10} on the lipid phase transition and, in particular, the minimal perturbation of the T_m by UQ_{10} (Figure 11) are not preserved in DMPC vesicles (Ulrich et al., 1983). UQ_2 and UQ_{10} in DMPC vesicles show differential accessibility to borohydride, but the difference is smaller than in DPPC vesicles (Table I). We suggest that the 14-carbon fatty acid chains of DMPC may be too short to insulate the UQ_{10} in the center of the bilayer from the membrane surface and that DPPC allows a better approximation to physiological membranes which contain lipid of even longer chain length. This difference in lipid chain length could explain the apparent contradiction between some of the results presented here and those of Kingsley & Feigenson (1981). Using ^1H NMR, they found that both UQ_1 and UQ_{10} in DMPC vesicles were accessible to lanthanide shift reagents. Furthermore, they could not observe the expected splitting of the quinone head-group resonances into two signals on addition of the lanthanides. Their interpretation was that the quinones were exchanging across the membrane quickly (on the NMR time scale), and using the maximum observed shift, they calculated minimum exchange rates large enough to be kinetically competent for electron transfer. We suggest that similar results would be expected if UQ_{10} were near the center of the bilayer, but the bilayer was thin enough for the shift reagents to penetrate a significant distance into it. This is likely since a broadening reagent has been shown to affect the protons on the methylenes and terminal methyls of the lipid acyl chains (Schuh et al., 1982). This kind of difference in structure of DPPC and the shorter chain DMPC vesicles is also illustrated by UQ_{10} causing the same T_m shift in the DMPC vesicles as did UQ_2 and UQ_3 (Ulrich et al., 1982). In vesicles made of longer chain length lipids such as DPPC, we would predict smaller maximum lanthanide-induced shifts and probably a splitting of the resonance from the more slowly exchanging UQ_2. In agreement with the present work, the data of Kingsley & Feigenson (1981) indicate that the quinones with longer chain lengths tend to be deeper in the bilayer, as their lanthanide-induced shifts are smaller than those for shorter chain quinones.

Kingsley & Feigenson (1981) also observed the existence in DMPC vesicles of the high-field $\sim$3.78 ppm resonance which they associated with methoxy protons of long-chain quinones. They ruled out the following explanations: (i) an impurity in UQ_{10}; (ii) a chemical change of UQ_{10} during preparation of the vesicles; and (iii) a pool of reduced UQ_{10}. It was proposed that the high-field signal arises from a separate vesicle population with a high quinone:phospholipid ratio. Our interpretation differs on the last point. We conclude that the 3.78 ppm high-field resonance arises from long-chain quinone in a concentrated more mobile environment located mainly in the center of the lipid bilayer because of (i) the homogeneity of the vesicle population (Figure 1), (ii) the lack of a high-field methoxy ($-OCH_3$) resonance in vesicles with surface-located UQ_2 or UQ_3 (Figure 6C), (iii) the larger amount of the high-field (3.78 ppm) peak in DPPC vesicles where UQ_{10} is more shielded from the surface (Figures 6D, 7, and 8), and (iv) the relative insensitivity of the chemical shift of this peak upon $NaBH_4$ reduction (Figure 9).

Exchange of quinone between the pool characterized by the more narrow peak at 3.78 ppm and the other quinone pool (3.93 ppm), whose average magnetic environment is similar to that of UQ_2, is very slow ($t_{1/2} >> 14$ ms). UQ_{10} present in the latter environment in DMPC vesicles has a strong effect on the lipid phase transition temperature, as does UQ_2 or UQ_3. In DPPC vesicles below the T_m, only 20% of the UQ_{10} methoxy groups are found in the UQ_2-like environment, while 80% are located in the more mobile or concentrated environment (Figure 8B). The UQ_{10} resonances do not freeze out below the vesicle T_m (Figure 10), and UQ_{10} does not have a large effect on the T_m of DPPC vesicles (Figure 11). These data are all consistent with the placement of a significant fraction of UQ_{10} in a mobile pool near the center of the DPPC bilayer. Tomkiewicz & Corker (1975) observed a similar phenomenon for the spin-label di-*tert*-butyl nitroxide incorporated into egg lecithin vesicles. Within the bilayer, the probe was in slow exchange between two environments with very different rotational times. They assigned the more mobile environment to the center of the bilayer and the other to some position nearer the lipid head groups.

From the combined UV–visible spectroscopic data on the extent and kinetics of quinone and ferricyanide reduction and the ^1H NMR analysis, we propose a model for the average or preferred location of short- and long-chain quinones in artificial lipid membranes. The readily reducible short-chain quinones such as UQ_2 are located near the outer surface of the bilayer and can cross the hydrophobic core only slowly to the inner surface. UQ_3 is slightly longer than UQ_2 and therefore is anchored more deeply in the bilayer. UQ_{10} is hydrophobic enough for a large fraction ($\sim$50% in Figures 2 and 3 at $T > T_m$) to be located in a mobile pool near the center of the lipid bilayer. Although this model does not exclude the possibility of motion of the centrally located long-chain quinone in a direction perpendicular to the plane of the membrane, it specifically excludes for the UQ_{10} in the center of the bilayer the kind of rapid flip-flop motion in which the long-chain quinones are thought to rapidly oscillate from contact with solvent at the outside of the membrane to that on the inside. We suggest that the special ability of the long-chain quinones to reconstitute energy transduction in depleted respiratory and photosynthetic membranes and to catalyze electron flow across model lipid membranes may correlate with the ability of these quinones to reside in the central region of the membrane. In biological membranes, donor and acceptor complexes such as the hemes of the *b* cytochromes (Widger et al., 1984) could serve to bring electrons close to the center of the bilayer where the quinone could serve to bridge the gap between them. Residence in the center of the lipid bilayer may also be necessary for carrying charges over long distances by lateral diffusion through a mobile phase (Anderson, 1981; Gupta et al., 1984).[2]

[2] The reader should also note a recent paper that has reached a different conclusion regarding the localization of UQ_{10} in bilayers (Stidham et al., 1984).

ACKNOWLEDGMENTS

We thank Prof. F. L. Crane for helpful discussions and Edward Bjes and Lucy Winchester for assistance in preparing the manuscript.

Registry No. UQ_{10}, 303-98-0; UQ_2, 606-06-4; UQ_3, 1173-76-8; DPPC, 2644-64-6; DMPC, 13699-48-4.

REFERENCES

Alonso, A., Gomez-Fernandez, J. C., Aranda, F. J., Belda, F. J. F., & Goñi, F. M. (1981) *FEBS Lett. 132*, 19–22.

Anderson, J. M. (1981) *FEBS Lett. 124*, 1–10.

Baccarini-Melandri, A., Gabellini, N., Melandri, B. A., Hurt, E., & Hauska, G. (1980) *J. Bioenerg. Biomembr. 12*, 95–110.

Barr, R., & Crane, F. L. (1971) *Methods Enzymol. 23*, 372–408.

Birdsall, N. T. M., Feeney, J., Lee, A. G., Levine, Y. K., & Metcalfe, J. C. (1972) *J. Chem. Soc., Perkin Trans. 2*, 1441–1445.

Brown, J. B., & Svensson, M. (1957) *J. Am. Chem. Soc. 79*, 4241–4242.

Chance, B., DeVault, D. C., Frauenfelder, H., Marcus, R. A., Shrieffer, J. R., & Sutin, N. (1979) in *Tunneling in Biological Systems*, pp 595–603, Academic Press, New York.

Crane, F. L. (1977) *Annu. Rev. Biochem. 46*, 439–469.

Crane, F. L., & Ehrlich, B. (1960) *Arch. Biochem. Biophys. 89*, 134–138.

De Pierre, J. W., & Ernster, L. (1977) *Annu. Rev. Biochem. 46*, 201–262.

Eigenberg, K. E., & Chan, S. T. (1980) *Biochim. Biophys. Acta 599*, 330–335.

Futami, A., & Hauska, G. (1979) *Biochim. Biophys. Acta 547*, 597–608.

Futami, A., Hurt, E., & Hauska, G. (1979) *Biochim. Biophys. Acta 547*, 583–596.

Gupta, S., Wu, E.-S., Hoechli, L., Hoechli, M., Jacobson, K., Sowers, A. E., & Hackenbrock, C. R. (1984) *Proc. Natl. Acad. Sci. U.S.A. 81*, 2606–2610.

Hauska, G., & Hurt, E. (1982) in *Function of Quinones in Energy Conserving Systems* (Trumpower, B., Ed.) pp 87–110, Academic Press, New York.

House, H. O. (1972) *Modern Synthetic Reactions*, pp 49–54, W. A. Benjamin, Menlo Park, CA.

Jain, K. M., & Wu, N. M. (1977) *J. Membr. Biol. 34*, 157–201.

Katsikas, H., & Quinn, P. J. (1981) *FEBS Lett. 133*, 230–234.

Katsikas, H., & Quinn, P. J. (1982) *Biochim. Biophys. Acta 689*, 363–369.

Kingsley, P. B., & Feigenson, G. W. (1979) *FEBS Lett. 97*, 175–178.

Kingsley, P. B., & Feigenson, G. W. (1981) *Biochim. Biophys. Acta 635*, 602–618.

Kostelnik, R. J., & Castellano, S. M. (1973) *J. Magn. Reson. 9*, 291–295.

Lambeth, D. O., & Palmer, G. (1973) *J. Biol. Chem. 248*, 6095–6103.

Lenaz, G., Esposti, M. O., Fata, R., & Cabrini, L. (1981) in *Biomedical and Clinical Aspects of Coenzyme Q* (Folkers, K., & Yamamura, Y., Eds.) Vol. 3, pp 169–182, Elsevier/North-Holland Biomedical Press, Amsterdam.

Mitchell, P. (1966) *Biol. Rev. Cambridge Philos. Soc. 41*, 445–502.

Mitchell, P. (1976) *J. Theor. Biol. 62*, 327–367.

Moret, V., Pinamonti, S., & Fornasari, E. (1961) *Biochim. Biophys. Acta 54*, 381–383.

Poulos, T. L., & Kraut, J. (1980) *J. Biol. Chem. 255*, 10322–10330.

Quinn, P. J., & Esfahani, M. A. (1980) *Biochem. J. 185*, 715–722.

Rouser, G., Siakatos, A. N., & Fleischer, S. (1966) *Lipids 1*, 85–86.

Schuh, J. R., Banerjee, U., Müller, L., & Chan, S. I. (1982) *Biochim. Biophys. Acta 687*, 219–225.

Seelig, J. (1977) *Q. Rev. Biophys. 10*, 363–418.

Sheetz, M. P., & Chan, S. I. (1972) *Biochemistry 11*, 4573–4581.

Stidham, M. A., McIntosh, T. J., & Siedow, J. N. (1984) *Biochim. Biophys. Acta 767*, 423–431.

Stockton, G. W., Polnaszek, C. F., Tullock, A. P., Hasan, F., & Smith, I. C. P. (1976) *Biochemistry 15*, 954–966.

Stroobant, P., & Kaback, H. R. (1979) *Biochemistry 18*, 226–231.

Tomkiewicz, M., & Corker, G. A. (1975) *Biochim. Biophys. Acta 406*, 197–205.

Trumpower, B. L. (1981) *J. Bioenerg. Biomembr. 13*, 1–24.

Tsukida, K. (1972) *Vitamins (Japan) 46*, 1–18.

Ulrich, E. L., Girvin, M. E., Markley, J. L., & Cramer, W. A. (1982) *Biophys J. 37*, 403a.

Ulrich, E. L., Girvin, M. E., Cramer, W. A., & Markley, J. L. (1983) *Biophys. J. 41*, 325a.

Van Geet, A. L. (1968) *Anal. Chem. 40*, 2227–2229.

Widger, W. R., Cramer, W. A., Herrmann, R. G., & Trebst, A. (1981) *Proc. Natl. Acad. Sci. U.S.A. 81*, 674–678.